Recombinant Kringle IV-10 Modules of Human Apolipoprotein(a): Structure, Ligand Binding Modes, and Biological Relevance†

Igor Mochalkin,‡ Beisong Cheng,‡ Olga Klezovitch,§ Angelo M. Scanu,*,§ and Alexander Tulinsky*,‡

Department of Chemistry, Michigan State University, East Lansing, Michigan 48824, and Department of Medicine and Department of Biochemistry and Molecular Biology, University of Chicago, 5841 South Maryland MC5041, Chicago, Illinois 60637

Received August 25, 1998; Revised Manuscript Received November 16, 1998

ABSTRACT: The kringle modules of apolipoprotein(a) [apo(a)] of lipoprotein(a) [Lp(a)] are highly homologous with kringle 4 of plasminogen (75−94%) and like the latter are autonomous structural and functional units. Apo(a) contains 14−37 kringle 4 (KIV) repeats distributed into 10 classes (1−10). Lp(a) binds lysine−Sepharose via a lysine binding site (LBS) located in KIV-10 (88% homology with plasminogen K4). However, the W72R substitution that occurs in rhesus monkeys and occasionally in humans leads to impaired lysine binding capacity of KIV-10 and Lp(a). The foregoing has been investigated by determining the structures of KIV-10/M66 (M66 variant) in its unliganded and ligand [ϵ-aminocaproic acid (EACA)] bound modes and the structure of recombinant KIV-10/M66R72 (the W72R mutant). In addition, the EACA liganded structure of a sequence polymorph (M66T in about 42−50% of the human population) was reexamined (KIV-10/T66/EACA). The KIV-10/M66, KIV-10/M66/EACA, and KIV-10/T66/EACA molecular structures are highly isostructural, indicating that the LBS of the kringles is preformed anticipating ligand binding. A displacement of three water molecules from the EACA binding groove and a movement of R35 bringing the guanidinium group close to the carboxylate of EACA to assist R71 in stabilizing the anionic group of the ligand are the only changes accompanying ligand binding. Both EACA structures were in the embedded binding mode utilizing all three binding centers (anionic, hydrophobic, cationic) like plasminogen kringles 1 and 4. The KIV-10/T66/EACA structure determined in this work differs from one previously reported [Mikol, V., Lo Grasso, P. V. and, Boettcher, B. R. (1996) *J. Mol. Biol. 256*, 751−761], which crystallized in a different crystal system and displayed an unbound binding mode, where only the amino group of EACA interacted with the anionic center of the LBS. The remainder of the ligand extended into solvent perpendicular to the kringle surface, leaving the hydrophobic pocket and the cationic center of the LBS unoccupied. The structure of recombinant KIV-10/M66R72 shows that R72 extends along the ligand binding groove parallel to the expected position of EACA toward the anionic center (D55/D57) and makes a salt bridge with D57. Thus, the R72 side chain mimics ligand binding, and loss of binding ability is the result of steric blockage of the LBS by R72 physically occupying part of the site. The rhesus monkey lysine binding impairment is compared with that of chimpanzee where KIV-10 has been shown to have a D57N mutation instead.

In human subjects, high plasma levels of lipoprotein(a) [Lp(a)][1] have been correlated with a high incidence of atherosclerotic cardiovascular disease *(1−4)*. Lp(a) is a special class of LDL having as a protein moiety apo(a) covalently linked to apoB100 by a disulfide bond *(5, 6)*. The primary sequence of apo(a) shares a remarkable degree of homology with that of plasminogen *(7, 8)*. Plasminogen, a major protein of the fibrinolytic system, consists of an array of five different kringle units (K1−K5) followed by a protease domain that contains the catalytic triad of serine proteases *(9)*. Apo(a) lacks the first three kringles of plasminogen and contains from 14 to 37 kringle 4-like repeats, referred to as KIV, distributed into 10 classes designated 1 to 10, exhibiting 75−94% sequence homology with plasminogen K4. KIV-9 contains an unpaired cysteine (Cys4057) that links apo(a) to one of the unpaired cysteines (Cys4326) in the C-terminal domain of apoB100 *(10, 11)*. KIV-10 is followed by one copy of KV and a protease domain, which have 91% and 94% sequence homology with K5 and the catalytic domain of plasminogen, respectively *(7)*.

Plasminogen is known to bind lysine−Sepharose via the LBS located in the K1 and K4 modules *(12)*. Lp(a) also binds

† Supported by NIH Grant HL 25942 (A.T.) and Program Project Grant HL 18577 (A.M.S.).

* To whom correspondence should be addressed.

‡ Michigan State University.

§ University of Chicago.

[1] Abbreviations: Lp(a), lipoprotein(a); LDL, low-density lipoprotein; apo(a), apolipoprotein(a); apoB100, apolipoprotein B100; K1 to K5, the kringle 1 to kringle 5 (residues C^{84}−C^{541}) regions of human plasminogen; KIV and KV, the kringle 4 and kringle 5 regions of apo(a); KIV-1, KIV-2, ..., KIV-10, KIV modules, type 1−10; LBS, lysine binding site; PTK1, kringle 1 of prothrombin; uPA, urokinase plasminogen activator; t-PA, tissue-type plasminogen activator; EACA, ϵ-aminocaproic acid; KIV-10/T66, KIV-10/M66, sequence polymorphs of KIV-10; K_d, dissociation constant; 5-Apa, 5-aminopentanoic acid; 7-Aha, 7-aminoheptanoic acid; KIV-10/M66R72, W72R mutant; KIV-10/N57, D57N mutant of chimpanzee.

10.1021/bi9820558 CCC: $18.00
Published on Web 01/27/1999

lysine−Sepharose *(8)* but via the LBS located in apo(a) KIV-10. This information has been derived from studies of defective lysine binding Lp(a) species from rhesus monkeys *(13)* and the human R72 mutant *(14)* as well as wild-type (W72) and mutant (R72) KIV-10 individually expressed in *Escherichia coli (15, 16)*. The critical role of W72 in lysine binding, which has emerged from the above observations, is consistent with the results of the structure of PTK1 *(17)*, which has an R in position 72. This residue extends diagonally across the region equivalent to the LBS, occupying it and sterically precluding binding of lysine-like ligands. The same notion also emerges from the modeling of the LBS of rhesus *(13)* and human mutant *(18)* KIV-10.

Recently, Chenivasse et al. *(19)* reported that the C-terminal region of apo(a) of chimpanzee *(Pan troglodytes)* exhibits a high degree of homology with the corresponding region of human apo(a). In turn, chimpanzee apo(a) differed from the rhesus counterpart by having (1) an intact catalytic triad in the protease region, (2) one copy of the KV motif, and (3) W in position 72 in the LBS of KIV-10. However, like the rhesus product, chimpanzee Lp(a) was deficient in lysine binding, a functional impairment attributed to the presence of N instead of D in position 57 in KIV-10 *(19)*. A sequence polymorphism, M66T, in apo(a) KIV-10 has also been reported in 42−50% of the human population *(20, 21)*. This mutation, however, is silent and causes no lysine binding deficiency in Lp(a).

The kringles of apo(a), like those of plasminogen, are autonomous structural and functional modular units that consist of a characteristic triple loop structure of approximately 80 amino acids cross-linked by three disulfide bridges in the pattern 1−6, 2−4, and 3−5. Kringle units are also present in the noncatalytic region of a variety of other distinct proteins involved in blood coagulation and fibrinolysis. A single copy of a kringle exists in uPA, vampire bat plasminogen activator, and factor XII, while kringles are found as pairs in prothrombin and t-PA and as quartets in hepatocyte growth factor *(22)*. The LBS of kringles, important in molecular recognition, binds lysine residues of several different proteins, such as fibrin, α2-antiplasmin, tetranectin, and thrombospondin. These kringle-dependent interactions can be competitively inhibited by lysine zwitterionic analogues such as EACA, benzamidine, *trans*-(4-aminomethyl)-cyclohexane-1-carboxylic acid and *p*-(aminomethyl)benzoic acid. Three-dimensional structures of uncomplexed and liganded kringle domains of most of the foregoing kringles have been determined by X-ray crystallography (ref *23* and references therein) and by NMR methods *(24, 25)*.

The LBS of plasminogen K1 *(23, 26)* and K4 *(27, 28)* is characterized by short arrays of residues H33−R35 (H33−K35 in K4), D55−D57, W62−F64, and R71−Y74, which together are arranged in a relatively open elongated surface depression approximately 9 Å wide and 12 Å long. Residues W62, F64, W72, and Y74 form a hydrophobic pocket bounded by a negatively charged anionic subsite containing D55 and D57 at the top and a positively charged cationic one containing R35 or K35 and R71 at the bottom. The anionic and cationic centers of the LBS stabilize the amino and carboxylic groups of ligands *(23, 28)*. The hydrophobic pocket interacts with the methylene chain of ω-amino acids so that all three binding centers of the LBS are simultaneously operative in an unrestricted way.

An unexpected binding mode was observed in KIV-10/T66 complexed with EACA *(29)* by the crystallography group at Sandoz Pharma AG, Basel, Switzerland.[2] In this case, only the ε-amino group of the zwitterionic ligand was reported to interact with the anionic binding center of the kringle while the remainder of the ligand extended into the solvent region, almost perpendicular to the surface of the kringle, leaving the cationic site and the hydrophobic pocket unoccupied. This binding mode (hereinafter called unbounded) and the corresponding structure might be expected with plasminogen K5 where the R35I and R71L substitutions in the LBS remove the cationic site of the kringle and could thus force a ligand to solely occupy the anionic binding site with a correspondingly larger K_d (140 μM) *(30)*. The unbounded binding mode of KIV-10/T66/EACA *(29)*, however, is not consistent with biochemical studies, which clearly suggest the embedded binding mode displayed by K1 and K4 *(23, 28)*. All three binding centers are present in KIV-10/T66, and the K_d value of EACA ($K_d = 20$ μM) is similar to those of plasminogen K1 ($K_d = 13$ μM) and K4 ($K_d = 48$ μM) *(15)*. Furthermore, the K_d values of ligands in the unbound mode should not differ significantly with the length of the ligand because only the terminal ε-amino group interacts with the anionic center. The measured dissociation constants of KIV-10/T66 with 5-Apa ($K_d = 66$ μM), EACA ($K_d = 20$ μM), and 7-Aha ($K_d = 230$ μM) *(15)* suggest otherwise and the embedded binding mode.

These anomalies and inconsistencies led us to reinvestigate the binding mode of EACA in the LBS of human KIV-10/T66 during the course of a more extensive study of the structures of the KIV-10/M66 variant in its free and ligand-bound states, as well as determine the structure of the human apo(a) KIV-10/M66R72 mutant. We report here highly refined, high-resolution structures of these apo(a) kringles that show (1) KIV-10/T66 can bind EACA in the embedded way, (2) in KIV-10/M66R72, the arginine mutation occupies the LBS mimicking ligand, and (3) R35 shifts on EACA binding to assist R71 at the cationic center. The various KIV-10 structures are also compared and their LBS correlated.

MATERIALS AND METHODS

Expression of Apo KIV-10/M66W72 and R72 in E. coli. The KIV-10/T66 expressed in *E. coli (15)* was provided by Dr. B. R. Boettcher of Novartis Pharmaceuticals Corp., Summit, NJ. The kringle contained four nonkringle amino acid residues (GSHM) resulting from the expression construct in addition to three residues (VRQ) preceding C^1 of KIV-10 and seven residues (SDTEGTV) downstream from C^{80} of KIV-10.

KIV-10/M66 and mutant KIV-10/M66R72 were expressed in *E. coli* as described previously *(16)* except that the PCR primers C and F were replaced by primers 5′-CCGGG-GATCCCGGCAGTGCTACCAT-3′ and 5′-CCGGGAAT-TCTTACACAGTCCCTTC-3′, respectively, to minimize the number of nonkringle residues. The DNA fragments that code for KIV-10/M66 and KIV-10/M66R72 were cloned into the *Bam*HI- and *Eco*RI-digested vector pGEX-KG, which was driven by the *tac* promoter and contained the coding

[2] Sandoz Corp. is now Novartis Corp.

Table 1: Conditions Used To Crystallize the Various Kringles[a]

	KIV-10/M66	KIV-10/M66/EACA	KIV-10/*T*66/EACA	KIV-10/M66R72
protein concn	20 mg/mL	20 mg/mL 10-fold molar excess of EACA	24 mg/mL 10-fold molar excess of EACA	20 mg/mL
precipitant	10% acetone, 15% PEG 8000, 0.1 M HEPES, 0.1 M Li_2SO_4, pH 7.0	20% 2-propanol, 20% PEG 4000, 0.1 M sodium citrate, pH 5.6	20% 2-propanol, 20% PEG 4000, 0.1 M sodium citrate, pH 5.6	20% PEG 8000, 0.1 M sodium cacodylate, 0.1 M Li_2SO_4, pH 6.5
crystal dimensions	0.18 × 0.15 × 0.02 mm	0.23 × 0.13 × 0.02 mm	0.50 × 0.10 × 0.02 mm	0.45 × 0.15 × 0.04 mm
cryo condition	20% PEG 8000, 20% glycerol, 0.1 M HEPES, pH 7.0	20% PEG 4000, 20% glycerol, 0.1 M sodium citrate, pH 5.5	20% PEG 4000, 20% glycerol, 0.1 M sodium citrate, pH 5.5	20% PEG 8000, 20% glycerol, 0.1 M sodium cacodylate, pH 6.5

[a] 2.0 μL hanging drop consists of 50% protein/50% precipitant solution suspended over 0.75 mL of the latter.

Table 2: Crystal Data and Intensity Data Collection Statistics of Different KIV-10 Crystals

	KIV-10/M66	KIV-10/M66/EACA	KIV-10/*T*66/EACA	KIV-10/M66R72
space group	$P2_12_12_1$	$P2_12_12_1$	$P2_12_12_1$	$P2_12_12_1$
cell constant (Å)				
a	24.61	24.37	24.30	24.30
b	45.68	45.60	45.67	45.82
c	63.70	62.90	63.36	56.23
resolution (Å)	2.07	1.78	1.80	2.20
independent reflections	3822	5717	5656	2241
redundancy	2.5	2.6	2.5	2.9
observations	9644	14679[a]	12758	6494
R-merge (%)	6.2	5.7	6.0	8.9
R-merge (%), outermost range (Å)	15.3 (2.25−2.07)	9.3 (2.00−1.78)	10.1 (2.00−1.80)	8.9 (2.50−2.20)
completeness (%)	81	79	81	63
outermost range (%)	64	53	53	45
I/σ outermost range	3.0	5.7	4.7	2.0

[a] $I/\sigma(I) > 1.5$; all others, $I/\sigma(I) > 1.0$.

sequence for glutathione S-transferase (GST) *(31)*. DNA sequences of wild-type and mutant kringles were confirmed by using the femptomolar sequencing kit from Promega (Madison, WI) according to the manufacturer's instructions. The kringles were expressed in the *E. coli* strain DH5a as fusion GST proteins and separated from the GST fusion component as previously described *(16)*. N-Terminal protein sequencing of the expressed products was also performed as described elsewhere *(32)*. The expressed kringles contained two nonkringle residues (GS) resulting from the expression construct in addition to two residues (RQ) preceding C^1 of KIV-10 and seven residues (SDTEGTV) downstream C^{80} of KIV-10. Each of the expressed kringles gave a single band by SDS−PAGE and reacted against an anti-apo(a) KIV-10 polyclonal antibody *(16)*. The kringles were extensively dialyzed against 1 mM NH_4HCO_3, lyophilized, and stored at −80 °C before use.

Crystallization. Relatively large crystals of the KIV variant, with and without EACA, could be grown from ammonium sulfate−PEG 8000 solutions. Their X-ray diffraction patterns, however, showed a complex splitting pattern that could not be successfully interpreted and indexed. All indications suggested that the apparently single crystals were actually several small, similarly oriented, fused crystals. Consequently, hanging drops (2.0 μL) of Hampton factorial solutions were examined. Excellent X-ray quality single crystals of KIV-10/M66/EACA and KIV-10/T66/EACA[3] could be readily grown from Hampton condition 40 (Table 1). However, crystallization of the other two kringles was not successful with this condition. Previous experience with kringles suggested that PEG 8000 as precipitant in a buffer with pH around 7.0, with or without salt, might be suitable. An in-house set of factorial solutions based on the foregoing was prepared and the hanging drop method applied again to the KIV-10/M66 and KIV-10/M66R72 samples. The conditions were eventually refined to produce X-ray quality single crystals. The crystallization conditions of all the KIV-10 kringles are given in Table 1.

Intensity Data Collection. The X-ray diffraction data of the KIV-10 crystals were measured with an R-AXIS II imaging plate detector using Molecular Structure Corporation−Yale focusing mirrors. The Cu Kα radiation was generated with a Rigaku RU200 rotating anode operating at 5 kW power with a fine focus filament (0.3 mm × 3.0 mm). Intensity data were measured at −150 °C with crystals flash frozen in a cryosolvent consisting of 20% PEG 4000/8000, 20% glycerol, and 0.1 M buffer that was also used in the crystallization (Table 1). The crystal−detector distance was 10.0 cm, and the detector−swing angles were 0° for KIV-10/M66 and KIV-10/M66R72, 8.0° for KIV-10/M66/EACA, and 10.0° for KIV-10/T66/EACA. Autoindexing and processing of the diffraction data were carried out with the Rigaku R-AXIS software package *(33)*, and the results are summarized in Table 2. Three of the crystals are isomorphous; the *c*-axis of the KIV-10/M66R72 mutant, however, shrank by about 7.0 Å.

Structure Determination. The crystal structure of KIV-10/T66/EACA was determined by molecular replacement using the coordinates of K4 of human plasminogen (PDB code: 1PK4) as an initial model. All residues of K4 that differed in sequence from KIV-10/T66 were replaced with

[3] Although the crystallization of unbounded KIV-10/T66/EACA was attempted following described procedures *(29)*, the crystals proved to be generally small and of marginal X-ray diffraction quality.

Table 3: Summary of Final Restrained Least-Squares Statistics

		RMSΔ			
crystal	target	KIV-10/M66	KIV-10/ M66/EACA	KIV-10/T66/EACA	KIV-10/M66R72
distances (Å)					
bond lengths	0.020	0.012	0.017	0.016	0.011
bond angles	0.040	0.032	0.039	0.039	0.032
planar 1−4	0.050	0.043	0.047	0.047	0.041
planes (Å)					
peptides	0.030	0.024	0.029	0.027	0.026
aromatic groups	0.030	0.029	0.037	0.034	0.029
chiral volumes (Å^3)	0.130	0.125	0.165	0.169	0.118
nonbonded contacts (Å)					
single torsion	0.60	0.18	0.18	0.20	0.22
multiple torsion	0.60	0.26	0.21	0.28	0.29
possible H-bond	0.60	0.32	0.24	0.32	0.28
thermal parameters (Å^2)					
main-chain bond	1.5	1.1	1.5	1.6	1.1
main-chain angle	2.0	1.8	1.8	2.2	1.7
side-chain bond	2.5	2.1	2.6	3.0	1.8
side-chain angle	3.0	3.0	3.3	3.5	2.5
range (Å)		9.0−2.1	9.0−1.8	9.0−1.8	9.0−2.1
R-value (%)		17.8	17.6	18.2	16.6
no. of water molecules[a]		67	77	109	41
⟨*B*⟩ (Å^2)		21.8	15.6	15.9	21.5
Cα rmsΔ (Å)[b]		/	0.30	0.30	0.43
PDB code		1KIV	2KIV	3KIV	4KIV

[a] Occupancy > 0.5. [b] Calculated versus KIV-10/M66.

alanine. Rotation/translation searches were conducted with the program AMoRe *(34)* in the resolution range 10.0−3.5 Å. The rotation search provided one distinct solution with a correlation coefficient of 0.30. The position of the molecule was fixed by a translation function that increased the correlation coefficient to 0.39 (R = 48.5%). Rigid body optimization further increased the correlation coefficient to 0.64 (R = 37.6%). Additional positional refinement by energy minimization in the 10.0−3.0 Å range to relieve close contacts of the model was carried out with the X-PLOR program package *(35)*, decreasing the *R*-value to 27.6%.

The crystal structure of KIV-10/T66 complexed with EACA was refined with the programs PROLSQ *(36)* and PROFFT *(37)*. First, three cycles of overall *B*-factor refinement starting with B = 18.0 Å^2 converged to an *R*-value at 32.9% (7.0−2.8 Å). Then three cycles of the individual temperature factor refinement brought the *R*-value to 29.4%. Further refinement applying alternate tight−loose geometry restraints decreased *R* to 28.3%. At this stage, $2F_o - F_c$ electron and $F_o - F_c$ difference density maps indicated most of the correct side chains of KIV-10/T66 that were alanine residues in the initial model and revealed EACA, which was not included in calculations. Further refinement was conducted including most of the actual residues of the kringle, as well as EACA. Solvent water molecules were added periodically on the basis of examination of difference density maps at 2.5 Å and higher resolution.

Since the crystals of KIV-10/M66 and KIV-10/M66/EACA are isomorphous with that of KIV-10/T66, the structure determinations of these two were conducted using isomorphous replacement methods. The refined coordinates of the KIV-10/T66 variant, with T66 replaced by alanine, were used as an initial model. Rigid body optimization with the X-PLOR program package in the 10.0−3.0 Å range decreased the *R*-value from 38.6% to 33.2% for unliganded KIV-10/M66 and from 43.7% to 34.5% for KIV-10/M66/EACA (without the ligand in the calculations). Additional positional refinement improved the *R*-values to 25.1% and 28.1%, respectively. After three cycles of overall *B*-factor refinement and three cycles of individual *B* refinement using the program PROFFT, *R* converged to 24.6% for KIV-10/M66 and 26.4% for KIV-10/M66/EACA. The $2F_o - F_c$ electron and $F_o - F_c$ difference density maps clearly showed M66 in KIV/M66 and the EACA in addition, in the KIV-10/M66/EACA structure.

The crystal structure of KIV-10/M66R72 had to be determined de novo by the molecular replacement method (because of the dramatic shrinkage of the *c*-axis, Table 2) using the coordinates of KIV-10 from the KIV-10/T66/EACA complex. Residues T66 and R72 were replaced with alanine, and EACA was omitted from the model. The rotation/translation search in the resolution range 10.0−3.0 Å provided one distinct solution with a correlation coefficient of 0.71 and a *R*-value of 32.6%, while further rigid body refinement decreased the *R*-factor to 30.5%. Final restrained least-squares parameters and *R*-factor statistics for the KIV-10 complexes are presented in Table 3.

RESULTS

The electron density is well defined for most of the residues of the kringle variants except the interkringle peptides that are disordered here and in other kringle structures. The rms deviations of the position of Cα atoms between the different KIV-10 units (about 70 Cα positions) indicate that the molecules exhibit very similar structural folding (Table 3). Ramachandran plots of the KIV-10 variants reveal that all non-glycine and non-proline residues, except M48, lie in the allowed regions. Similar to other kringle structures, plasminogen K1, K4, and their EACA derivatives, K5, and unbounded KIV-10/T66/EACA *(23, 26−30)*, the residue at position 48 has well-defined main- and side-chain electron density in all of them, corresponding to a hairpin turn, but is in a generously allowed area of the Ramachandran

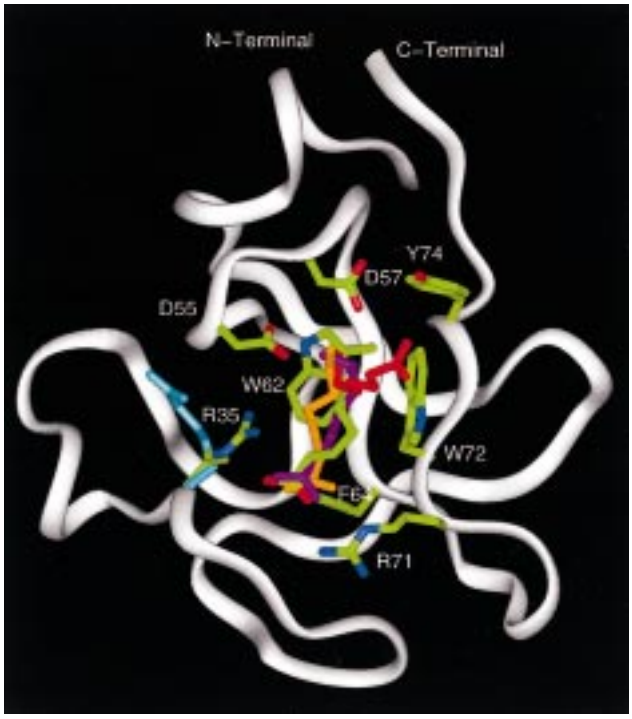

FIGURE 1: Superposition of EACA of different lysine binding kringles: embedded KIV-10/T66/EACA, carbon atoms in green, nitrogens in blue, and oxygens in red (atom colors); unbounded KIV-10/T66/EACA, red; plasminogen K1/EACA, orange; plasminogen K4/EACA, purple; embedded KIV-10/T66/EACA side chains, atom colors. The conformation of R35 in KIV-10/M66 is in all blue.

plot. No kringle residue was found in a disallowed region. As in other kringle structures, the P30 residue is in a cis conformation.

The LBS of KIV-10 is also defined by R32−R35, D55−D57, W62−F64, and R71−Y74 (Figure 1). Hydrogen bonds in the LBS region can be divided into three principal groups according to several factors, which can depend on the binding of EACA or on intermolecular interactions of neighboring molecules in crystals. The first group includes hydrogen bonds that are common to all the structures (Table 4). These interactions in the LBS mainly involve atoms of the backbone and are generally not completely exposed on the surface. The second group consists of the hydrogen bonds that result from the binding of EACA (Table 5). The residues of the anionic and cationic binding centers and several water molecules in the LBS participate in the hydrogen-bonding interactions of this group. Residue R32, which is located on the surface of the LBS, gives rise to the third group of hydrogen bonds in the LBS region that depend on crystal packing (Figure 2).

In the liganded structures of the M66 and T66 variants of KIV-10, the electron density of the EACA in the LBS is similar and well defined (Figure 2) and EACA interacts in the *embedded* way with all three binding centers in both kringles (Figures 1 − 3). The anionic (D55/D57) and cationic (R35/R71) centers stabilize the amino and carboxylic groups, respectively, while the hydrophobic pocket (W62, F64, W72, Y74) interacts with the methylene chain of the ligand. Thus, the KIV-10/T66/EACA structure determined here differs very significantly from the unbounded KIV-10/T66/EACA structure reported previously *(29)*, which only showed ligand binding at the anionic center (Figure 1). Except for Arg35, the binding of EACA to both the M66 and T66 variants occurs with minimal structural reorganization so the LBS appears to be essentially preformed anticipating ligand.

Because of the decrease of the lysine binding affinity of KIV-10/M66R72 compared to that of the T66 and M66 variants *(16)*, its LBS is of special interest. Substituting a nonaromatic amino acid for W72, an obviously important residue of the hydrophobic pocket along with W62 (Figure 3), would in itself be expected to lead to some impairment of binding affinity. The structure of KIV-10/M66R72 additionally shows that R72 extends across the LBS toward the negatively charged D55/D57 pair making a hydrogen bonded salt bridge with D57 (Table 5) and thusly obstructs access to the LBS. Since the cationic center consisting of R35 and R71 does not undergo any structural changes and is positionally similar to that of the unliganded KIV-10 molecule (Figures 1 and 3), the arginyl of R72 occupying the binding groove of the LBS appears to be the structural deterrent responsible for the lack of binding affinity of the KIV-10 mutant.

All four KIV-10 variants crystallized in the orthorhombic space group $P2_12_12_1$. Three of the crystals are isomorphous, while the *c*-axis of the fourth, KIV-10/M66R72, is about 7.0 Å shorter (Table 2). This 10% shrinkage is the result of different molecular packing of the KIV-10/M66R72 molecules along the *c*-axis of the crystal. Superposition of the mutant with any of the three isomorphous variants showed very little rotation of the molecules with respect of each other, with only a translational difference along the *z*-direction. In all four crystal arrangements, kringle molecules form infinite chain columns parallel to the *y*-direction with a 15 Å wide channel between chains. In KIV-10/M66R72, two neighboring symmetry-related molecules are aligned approximately 3.5 Å closer along the crystallographic *c*-axis, while the packing along the two other axes remains about the same. The net result is to shrink the channel to about 7 Å at the expense of solvent water molecules. The solvent fraction of the three isomorphous KIV-10 structures is approximately 30.6% ($V_M = 1.76$ Å^3/Da). In the case of the W72R mutant, the shrinkage along the *c*-axis decreases the solvent content to 22.0% ($V_M = 1.56$ Å^3/Da). The number of water molecules found in the four different kringle structures varies from 41 to 109 and is generally related to the resolution of the diffraction data, but in the case of KIV-10/M66R72, it depends primarily on the solvent fraction of the crystals.

DISCUSSION

The overall topology of human KIV-10 is an oblate ellipsoid of approximately 28 Å in diameter and 18 Å thick (Figure 1). The LBS of KIV-10 is similar to those of plasminogen K1 and K4 *(23, 26−28)*. All three key segments, the anionic, cationic, and hydrophobic centers, are essentially positioned optimally for ligand binding in KIV-10/M66 and, except for R35 (Figure 1), remain so on ligand binding in KIV-10/M66/EACA and KIV-10/T66/EACA. In KIV-10/M66, residue D55 is in the same orientation ($\chi_1 \approx 60°$) as in plasminogen K1 and K4. In plasminogen K5, however, D55 extends into the solvent region in a different orientation ($\chi_1 \approx 100°$) apparently nonconducive to ligand binding *(30)*. It has been suggested that the D55 residue of

Table 4: Probable Conserved Hydrogen Bonds (Å) in LBS of KIV-10

		KIV-10/M66	KIV-10/M66/EACA	KIV-10/T66/EACA	KIV-10/M66R72
Arg35-NH2	Pro54-O	3.00	*a*	*a*	3.20
Asn53-OD1	Asp55-OD1	2.59	2.85	3.02	3.76[c]
Asn53-OD1	Asp55-N	2.75	2.82	2.44	2.51
Asn53-ND2	Asp57-O	2.77	2.90	3.02	3.17
Asn53-ND2	Asn5-O	2.50	2.75	2.63	2.54
Asn53-OD1	Trp62-NE1	2.51	2.74	2.70	3.01
Asp57-OD1	Tyr74-OH	2.88	2.41	2.87	2.44
Asp57-OD1	Thr58-N	2.64	2.68	2.59	2.46
Asp57-OD2	O_w242/212/255[b]	3.60	3.06	2.96	*c*
Pro61-O	Cys75-N	3.00	2.85	2.94	3.43[c]
Pro61-O	O_w228/264/258[b]	2.72	2.74	3.23	*c*
Trp62-N	Arg52-O	2.77	2.81	2.95	2.66
Trp62-O	Arg52-N	3.50	3.11	3.06	3.45[c]
Cys63-N	Glu73-O	3.04	2.98	3.01	3.49[c]
Cys63-O	Glu73-N	3.03	2.99	3.15	3.37[c]
Phe64-N	O_w201/202/208/219[b]	2.73	2.88	2.74	2.58
Phe64-O	Gln23-N	2.61	2.64	2.69	3.38[c]
Arg71-O	Thr65-N	3.10	3.10	2.96	2.58
Arg71-NH1	Arg32-O	2.65	2.75	2.86	3.37[c]
Trp72-O	O_w222/249/239[b]	3.48	3.05	2.96	*c*
Tyr74-N	O_w219/237/306[b]	2.72	2.96	2.88	*c*
Tyr74-O	Val17-N	2.88	3.00	3.06	3.68[c]

[a] R35 undergoes a conformational change. [b] Numbering of water molecules in respective structures. [c] Due to the shrinkage of the *c*-axis of the mutant, the solvent content is reduced to 22% (total of 41 water molecules, Table 3), resulting in the loss of hydration interactions and some hydrogen bonds.

Table 5: Hydrogen Bonds (Å) in LBS of KIV Dependent on Ligand Binding and the W72R Mutation

kringle	ligand	KIV-10/ M66/EACA	KIV-10/ T66/EACA	KIV-10/ M66R72
Arg35-NE	EACA-OZ	2.98[a]	2.72[a]	
Arg35-NH1	O_w242/291	3.01	3.12	
Arg35-NH2	EACA-OZ	3.05	2.87	Pro54-O (3.20)
Arg35-NH2	Arg32-NH1[b]		2.67	3.22
Arg35-NH2	Arg32-NH2[b]			3.25
Pro54-O	O_w261/244	2.97	2.98	Arg35-NH2 (3.20)
Asp55-OD2	EACA-NZ	2.62	2.75	Arg32-NE (3.16)[a,b]
Asp57-OD2	EACA-NZ	2.53	2.87	Arg72-NH2 (3.01)
Arg71-NE	EACA-O	2.65[a]	3.13[a]	
Arg71-NH1	EACA-O	3.00	2.75	
Arg71-NH2				Thr29-OG1 (3.20)[b]

[a] Possibly a hydrogen bond. [b] Symmetry-related molecule.

K5 reorients on ligand binding to form a doubly charged anionic center along with D57, which then interacts with the amino group of the ligand as in KIV-10, K1, and K4. Thus, the LBS region of K5 possesses the anionic center, but with I35 and L71, it lacks the cationic one. It would therefore be expected that K5 can bind longer alkylamines such as 5- and 6-aminopentane and -aminohexane, respectively, which it does (*30*).

All three binding centers are operative in KIV-10/M66/EACA and KIV-10/T66/EACA examined in the present work, and EACA binds to the LBS in the embedded way (Figures 1 and 2). This binding mode, also observed in plasminogen K1 and K4 (Figure 1), is consistent with binding constants of different ligands discussed earlier. Thus, the binding of embedded KIV-10/T66/EACA is very different from the unbounded mode previously reported for the KIV-10/T66/EACA structure *(29)*. It is noteworthy, however, that lysine binding kringles can bind ligand in two different ways.

The source of the binding mode variance between our work and that of Mikol et al. *(29)* most likely resides in the different conditions used for crystallization. The major differences are as follows: unbounded KIV-10/T66/EACA, protein concentration 5 mg/mL, pH 7.5, in the presence of 40 mM NaCl; present work KIV-10/T66/EACA, 12 mg/mL, pH 5.6, no NaCl but with 10% 2-propanol and a 10-fold molar excess of EACA [latter unreported by Mikol et al. *(29)*]. Although the different pH conditions might seem important, liganded K1 and K4 crystals in the embedded mode were grown at higher pH values of 6.5 and 6.0, respectively.[4] It is of some note that, in the LBS of unliganded plasminogen K1 crystals, there are two chloride ions in the vicinity of the cationic center, which appear to interact with and neutralize R35 and R71 electrostatically *(26)*. In the case of unliganded plasminogen K4, the anion is a sulfate and the interaction is more complicated by the additional presence of a symmetry-related molecule *(27)*. Thus, it is conceivable that the unbound ligand binding mode of KIV-10/T66/EACA *(29)* could result because of an anion-compensated cationic center. However, examination of the *B*-values of the water molecules in the LBS of the latter reveals only evidence for water molecules of solvation (no inordinately small *B*-values evidencing anions).

The unique features of the LBS of the apo(a) KIV-10 of rhesus and chimpanzee are the point mutations that lead to an impairment in EACA binding and binding to lysine−Sepharose *(13, 16, 19)*. The structure of the recombinant mutant KIV-10/M66R72 shows that R72 extends along the ligand binding groove parallel to the expected position of EACA, toward the negatively charged D55/D57 anionic center, and makes a hydrogen-bonded salt bridge with D57 (Figure 3, Table 5). Thus, the R72 side chain mimics ligand binding, and loss of binding ability is the result of a steric blockage of the LBS by R72 physically occupying part of

[4] Mikol et al. crystallized unliganded KIV-10/T66 and KIV-10/T66/EACA (EACA in the unbounded binding mode) isomorphously (space group $P2_1$) *(29)*. Using practically the same conditions, however, they crystallized KIV-10/T66 liganded with *p*-(aminomethyl)benzoic acid in the embedded binding mode isomorphous (space group $P2_12_12_1$) with KIV-10/M66, KIV-10/M66/EACA, and KIV-10/*T*66/EACA of the present work.

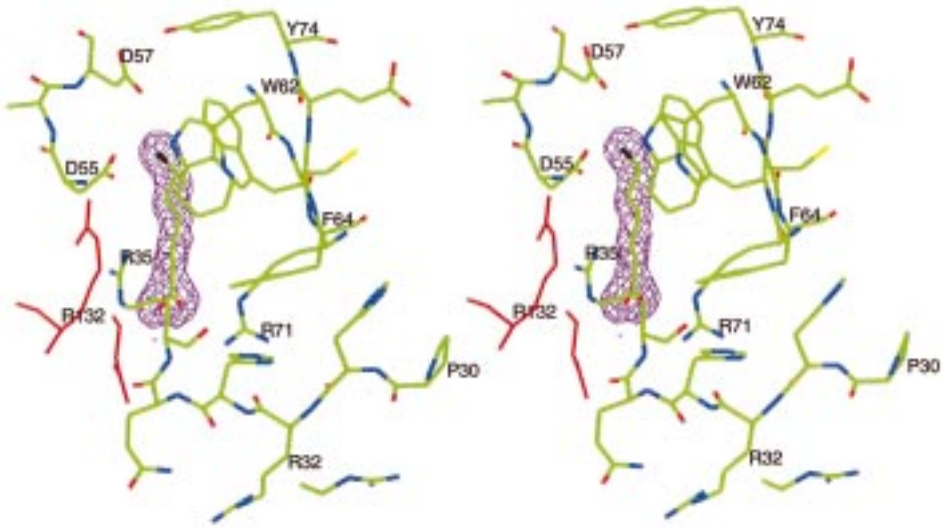

FIGURE 2: Stereoview of the final $2F_o - F_c$ electron density of EACA of KIV-10/T66/EACA displaying the embedded binding mode contoured in purple at 1σ. Two conformations of R32 are shown; R32 of the symmetry-related molecule (R132) is in all red.

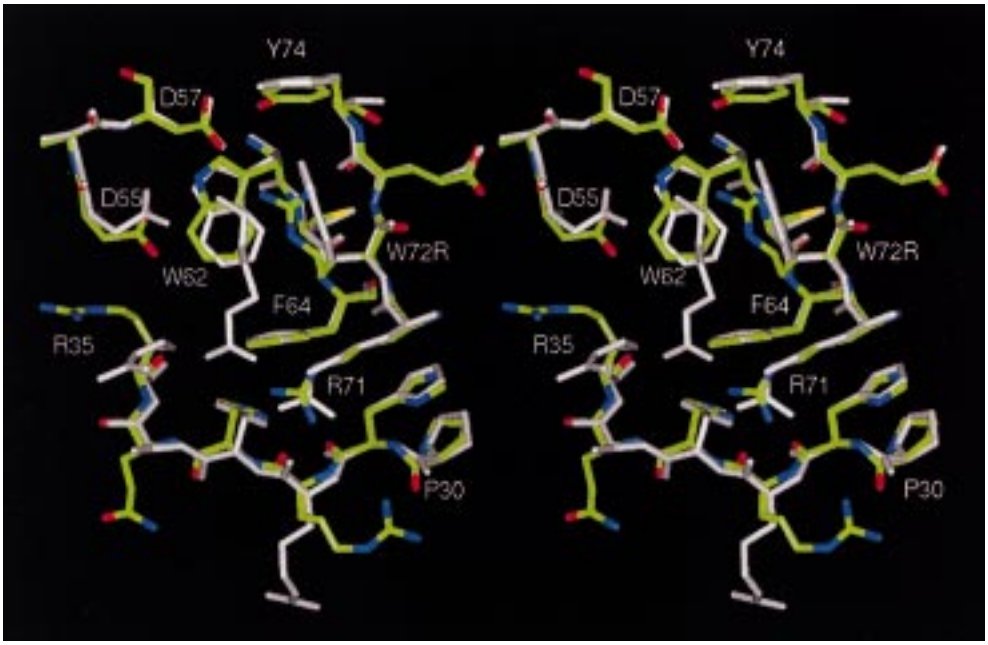

FIGURE 3: Stereoview of the superposition of KIV-10/M66R72 (atom colors) on KIV-10/M66/EACA (gray) showing R72 approximating EACA binding. Note the different conformation of R35 in the two structures.

the site. The LBS structure of KIV-10/M66R72 is similar to the LBS region of PTK1, which has an R72 equivalent but lacks the D57 to make a salt bridge. In this case, R72 appears to form a salt bridge with D55. This structure was used previously to model closely the LBS of rhesus KIV-10/M66R72 *(13)*. In turn, the D57N point mutation in the LBS of KIV-10/N57 of chimpanzee simply lowers the negative electrostatic charge of the anionic center that appears to be so critical for the binding of the quaternary, positively charged ϵ-amino group of lysine and other zwitterionic ligands. This only leads to an electrostatic impairment of an otherwise capable LBS. Since the N57 side chain is geometrically nearly isostructural with the D57 it replaces and can be a hydrogen bond donor or acceptor, it would seem that the LBS function of KIV-10 of chimpanzee should be less impaired compared to that of the rhesus monkey, primarily because the steric impairment of the latter excludes ligand physically. This suggested difference in LBS function between the KIV-10 of rhesus and chimpanzee could not be assessed further because the lysine binding conditions were not provided for the chimpanzee product *(19)*.

Superposition of the KIV-10/M66 and the ligand-bound KIV-10/M66/EACA and KIV-10/T66/EACA structures shows that the binding of EACA in KIV-10 is accompanied by (1) a displacement of water molecules from the EACA binding groove and (2) a movement of the arginyl residue of R35 (Figure 1). Three water molecules (O_w258, O_w259, O_w260) extending from the anionic to the cationic center in KIV-10/M66 are displaced by EACA with ligand binding. Two other hydrogen-bonding water sites, located in the LBS region but not in the EACA binding groove, are conserved in both structural types (Table 5). Similar to binding of EACA, the W72R mutation causes the displacement of water molecules from the binding groove. Additional examination of the residues within 5.0 Å of the LBS indicates only a conformational change in residue R35 on binding EACA.

In the ligand-free structures of KIV-10/M66 (Figure 1) and KIV-10/M66R72 (Figure 3), residue R35 adopts an extended conformation, almost parallel to the LBS groove, and utilizes a hydrogen bond with P54O (Table 4). Upon ligand binding, R35 of the M66 and T66 variants swings around the CA−CB bond by about −120° toward the cationic center but remains extended, bringing the guanidinium group close to the carboxylate of EACA to assist R71 in stabilizing the anionic end of the ligand (Figures 1, 2, and 3, Table 5) as in plasminogen K4. The movement is accompanied by an approximately 1.3 Å shift of the tyrosyl ring of the side chain of Y41 into the vacancy created by the R35 conformational change. When R35 is in the ligand binding posture, two water molecules (O_w261, O_w244; Table 5) also occupy the vacancy created by the shift. The KIV-10/T66/EACA also shows the arginyl reorientation but the guanidinium amino groups correspond to weaker electron density so their orientation is not as certain as that of the M66 variant.

Superposition of the KIV-10 variants also revealed different conformations for R32. This residue is located on the surface of the kringle and is adjacent to the LBS of a symmetry-related molecule and appears to play a role in molecular packing. The conformation of R32 is similar in the KIV-10/M66 and KIV-10/M66/EACA structures. In addition to a favorable hydrogen-bonding interaction between its carbonyl oxygen atom and R71NH1 in the free and ligand-bound structures (Table 4), the terminal guanidino nitrogen atoms of R32 in KIV-10/M66/EACA participate in a complicated electrostatic cluster comprised of the carboxyl group of EACA of the symmetry-related molecule and R35/D55 of the corresponding cationic and anionic binding centers. Apparent charge neutralization is achieved by the cluster through an pseudocyclic arrangement of positive and negative centers [*R*32 of a neighboring kringle, D55, quaternary amine of EACA, the carboxylate of EACA, and Arg35 (Figure 2)]. In the KIV-10/T66/EACA structure R32 has two alternate conformations, which have been refined to an occupancy of 0.6 (extended) and 0.4 (bent). The R32 in the extended conformation interacts with a symmetry-related kringle unit (Figure 2), whereas in the bent conformation it forms a hydrogen bond with cis P30O (3.00 Å) of the same molecule. An additional water molecule participates in the stabilization of both the extended and the bent conformation. In the KIV-10/M66R72 mutant, R32 is in an intermediate bent conformation displaying both intermolecular and intramolecular interactions while bridging two kringle molecules. The NH1 and NH2 atoms interact with cis P30O as in KIV-10/M66 and KIV-10/M66/EACA, but in addition, there are close intermolecular contacts between R32NE and D55OD2 (3.16 Å) as well as R32NH2 and R35NH2 (3.25 Å) of the LBS of a symmetry-related molecule.

The current crystallographic studies of a wild-type (W72) and mutant (R72) of human KIV-10 provide a detailed account of the way apo(a) KIV-10 binds to lysine and its analogues. This information is of biological relevance in that lysine binding and related activities of Lp(a) depend on the function of LBS of KIV-10 *(13, 14)*. The kringle, according to current dogma, is considered to be exposed because it has no apparent formal linkages with the lipoprotein component of Lp(a). In keeping with this notion is the lysine binding deficiency of rhesus monkey and the human mutant Lp(a) having the critical W72 replaced by R in the LBS of KIV-10. From the standpoint of the athero-thrombogenic potential of Lp(a), this type of mutation has been suggested to be benign on the premise that it would be unable to interfere with the plasminogen to plasmin conversion *(13, 14)*. This view has recently received support from studies with transgenic mice *(38)*. Because of the pathobiological significance of the LBS and its potential for mutability, it would be of further interest to study additional natural and/or artificial mutations in order to define their impact on the lysine binding activity of apo(a) KIV-10. In the current study we have shown that the replacement of M by T in position 66 had no significant structural consequences, in agreement with the finding that this common human mutation is functionally silent. The example provided by chimpanzee Lp(a) of a substitution at D55 by N is of interest in that we predict that such a substitution would lead to only a relatively modest degree of functional impairment of lysine binding function compared to that of the rhesus. A functional hierarchy in the LBS might account for the variability in lysine binding activity among human subjects based on measurements of whole plasma *(14, 39)*. In this context, however, we cannot rule out the contribution to the binding by a second LBS contained in the region between apo(a) KIV-5 and KIV-8 *(40)*. This region is usually open in free apo(a) whereas it is essentially masked when apo(a) is a constituent of the Lp(a) particle *(40, 41)*. A structural understanding of the region may be of some consequence in view of its suggested involvement in the lysine-mediated binding of apo(a) to fibrinogen *(42)*.

ACKNOWLEDGMENT

Writing of the paper was supported by a James L. Dye Endowed Fellowship and a Walter and Margaret Yates Memorial Scholarship (I.M.). We thank Dr. Brian R. Boettcher of Novartis Pharmaceuticals Corp., Summit, NJ, for providing us with the atomic coordinates and observed structure factors of unbounded KIV-10/T66/EACA *(29)*.

REFERENCES

1. Dahlen, G. H., Ericson, C., and Berg, K. (1978) *Clin. Genet. 14*, 36−42.
2. Kostner, G. M., Avogaro, P., Gazzolato G., Marth, E., Bittolo-Bon, G., and Qunici, G. B. (1981) *Atherosclerosis 38*, 51−61.
3. Murai, A. T., Miahara, T., Fujimoto, N., Matsuda, M., and Kameyama, M. (1986) *Atherosclerosis 59*, 199−204.
4. Dahlen, G. H., Guyton, J. R., Attar, M., Farmer, J. A., Kautz, J. A., and Gotto, A. M. (1986) *Circulation 74*, 758−765.
5. Brunner, C., Kraft H.-G., Utermann, G., and Müller H.-J. (1993) *Proc. Natl. Acad. Sci. U.S.A. 90*, 11643−11647.
6. Koschinsky, M. L., Côté, G. P., Gabel, B., and van der Hoek, Y. Y. (1993) *J. Biol. Chem. 268*, 19819−19825.
7. McLean, J. W., Tomlinson, J. E., Kuang, W.-J., Eaton, D. L., Chen, E. Y., Fless, G. M., Scanu, A. M., and Lawn, R. M. (1987) *Nature 330*, 132−137.
8. Eaton, D. L., Fless, G. M., Kohr, W. J., McLean, J. W., Xu, Q., Miller, C. G., Lawn, R. M., and Scanu, A. M. (1987) *Proc. Natl. Acad. Sci. U.S.A. 84*, 3224−3228.
9. Sottrup-Jensen, L., Clayes, H., Zajdal, M., Petersen, T. E., and Magnusson, S. (1978) *Prog. Chem. Fibrinolysis Thrombolysis 3*, 191−209.
10. Callow, M. J., and Rubin, E. M. (1995) *J. Biol. Chem. 270*, 23914−23917.
11. McCormick, S. P. A., Ng, J. K., Taylor, S., Flynn, L. M., Hammer, R. E., and Young, S. G. (1995) *Proc. Natl. Acad. Sci. U.S.A. 92*, 10147−10151.

12. Miles, L. A., and Plow, E. F. (1990) *Thromb. Haemostasis 63*, 331−335.
13. Scanu, A. M., Miles, L. A., Fless, G. M., Pfaffinger, D., Eisenbart, J., Jackson, E., Hoover-Plow, Brunck, T., and Plow, E. F. (1993) *J. Clin. Invest. 91*, 283−291.
14. Scanu, A. M., Pfaffinger, D., Lee, J. C., and Hinman J. (1994) *Biochim. Biophys. Acta 1227*, 41−45.
15. LoGrasso, P. V., Cornell-Kennon, S., and Boettcher, B. R. (1994) *J. Biol. Chem. 269*, 21820−21827.
16. Klezovitch, O., and Scanu, A. M. (1996) *Arterioscler., Thromb., Vasc. Biol. 16*, 392−398.
17. Tulinsky, A., Park, C. H., and Skrzypczak-Jankun, E. (1988) *J. Mol. Biol. 202*, 885−901.
18. Scanu, A. M., and Edelstein, C. (1995) *Biochim. Biophys. Acta 1256*, 1−12.
19. Chenivasse, X., Huby, T., Wickins, J., Chapman, J., and Thillet, J. (1998) *Biochemistry 37*, 7213−7223.
20. Kraft, H. G., Haibach, C., Lingenhel, A., Brunner, C., Trommsdorff, M., Kronenberg, F., Muller, H. J., and Utermann, G. (1995) *Hum. Genet. 95*, 275−282.
21. Scanu, A. M., Pfaffinger, D., Klezovitch, O., and Edelstein, C. (1995) in *Cardiovascular Disease* (Gallo, L. L., Ed.) Vol. 2, pp 45−47, Plenum Press, New York.
22. Nakamura, T., Nishizawa, T., Hagiya, M., Seki, T., Shimonishi, M., Sugimura, A., Tashiro, K., and Shimzu, S. (1989) *Nature 342*, 440−443.
23. Mathews, I. I., Vanderhoff-Hanaver, P., Castellino, F. J., and Tulinsky, A. (1996) *Biochemistry 35*, 2567−2576.
24. Rejante, M. R., and Llinas, M. (1994) *Eur. J. Biochem. 221*, 927−937.
25. Rejante, M. R., and Llinas, M. (1994) *Eur. J. Biochem. 221*, 939−949.
26. Wu, T.-P., Padmanabhan, K. P., and Tulinsky, A. (1994) *Blood Coagulation Fibrinolysis 5*, 157−166.
27. Mulichak, A. M., Tulinsky, A., and Ravichandran, K. G. (1991) *Biochemistry 30*, 10576−10588.
28. Wu, T.-P., Padmanabhan, K., Tulinsky, A., and Mulichak, A. (1991) *Biochemistry 30*, 10589−10594.
29. Mikol, V., LoGrasso, P. V., and Boettcher, B. R. (1996) *J. Mol. Biol. 256*, 751−761.
30. Chang, Y., Mochalkin, I., McCance, S. G., Cheng, B., Tulinsky, A., and Castellino, F. (1998) *Biochemistry 37*, 3258−3271.
31. Guan, K., and Dixon, J. E. (1991) *Anal. Biochem. 192*, 262−267.
32. Edelstein, C., Italia, J. A., and Scanu, A. M. (1997) *J. Biol. Chem. 272*, 11079−11087.
33. Higashi, T. (1990) *Appl. Crystallogr. 23*, 252−257.
34. Navaza, J. (1994) *Acta Crystallogr. A50*, 157−163.
35. Brunger, A. T. (1990) *X-PLOR, Version 3.1. A System for X-ray Crystallography and NMR*, Yale University Press, New Haven, CT.
36. Hendrickson, W. A. (1985) *Methods Enzymol. 115*, 252−270.
37. Finzel, B. C. (1987) *J. Appl. Crystallogr. 20*, 53−55.
38. Hughes, S. D., Lou, X. J., Ighani, S., Verstuyft, J., Grainger, D. J., Lawn, R. M., and Rubin, E. M. (1997) *J. Clin. Invest. 100*, 1493−1500.
39. Hoover-Plow, J. L., Boonmark, N., Skocir, P., Lawn, R. M., and Plow, E. F. (1996) *Arterioscler., Thromb., Vasc. Biol. 16*, 656−664.
40. Edelstein, C., Mandala, M., Pfaffinger, D., and Scanu, A. M. (1995) *Biochemistry 34*, 16483−16492.
41. Ernst, A., Helmhold, M., Brunner, C., Pethoschramm, A., Armstrong, V. W., and Muller, H. J. (1995) *J. Biol. Chem. 270*, 6227−6234.
42. Klezovitch, O., Edelstein, C., and Scanu, A. M. (1996) *J. Clin. Invest. 98*, 185−191.

BI9820558